

To Appear on The Astronomical Journal

**A k -NN Method to Classify Rare Astronomical Sources:
Photometric Search of Brown Dwarfs with *Spitzer*/IRAC**

Massimo Marengo

Harvard-Smithsonian Center for Astrophysics, 60 Garden St, Cambridge, MA 02138

`mmarengo@cfa.harvard.edu`

and

Mayly C. Sanchez¹

Argonne National Laboratory, 9700 South Cass Avenue, Argonne, IL 60439

`mayly.sanchez@anl.gov`

ABSTRACT

We present a statistical method for the photometric search of rare astronomical sources based on the weighted k -NN method. A metric is defined in a multi-dimensional color-magnitude space based only on the photometric properties of template sources and the photometric uncertainties of both templates and data, without the need to define ad-hoc color and magnitude cuts which could bias the search. The metric is defined as a function of two parameters, the number of neighbors k and a threshold distance D_{th} that can be optimized for maximum selection efficiency and completeness. We apply the method to the search of L and T dwarfs in the *Spitzer* Extragalactic First Look Survey and the Boötes field of the *Spitzer* Shallow Survey, as well as to the search of sub-stellar mass companions around nearby stars. With high level of completeness, we confirm the absence of late-T dwarfs detected in at least two bands in the First Look Survey, and only one in the Shallow Survey (previously discovered by Stern et al. 2007). This result is in agreement with the expected statistics for late-T dwarfs. One L/early-T candidate is found in the First Look Survey, and 3 in the Shallow Surveys, currently undergoing follow-up spectroscopic verification. Finally, we discuss the potential for brown dwarf searches with this method in the *Spitzer* warm mission Exploration Science programs.

Subject headings: methods: statistical — stars: brown dwarfs — infrared: stars

¹Department of Physics, Harvard University, 17 Oxford Street, Cambridge, MA 02138

1. Introduction

One of the most common problems in astrophysics is the classification of astronomical sources based on their colors and magnitudes in a given photometric system. When high spectral resolution data (or a large number of photometric bands covering the source SED) are available, this classification, and the extraction of the physical parameters of the source, is generally achieved by fitting the observations with an appropriate physical model. In many instances, however, either a reliable model is not available, or the number of photometric bands is not sufficient to provide a robust source classification. When data fitting is not possible, a common fallback solution is to infer the nature of the sources to be classified by their proximity to “regions” in meaningful color-color and color-magnitude diagrams, where the sources of a certain class are expected to be found.

These regions are in turn defined on the basis of generic physical considerations (e.g. stars burning H in their cores are located on the region of the Hertzsprung-Russell diagram we call Main Sequence) or by association with other sources of the same class. A typical example of this approach in the early years of infrared space astronomy were the IRAS color-color diagrams (van der Veen & Habing 1988) aimed to automatically classify the $2.4 \cdot 10^5$ sources found by the InfraRed Astronomical Satellite in its bands at 12, 25, 60 and 100 μm . The diagrams were created by deriving the IRAS colors of $\sim 5,400$ sources whose nature could be inferred by the properties of their IRAS Low Resolution Spectra (LRS 1986). The resulting diagrams were a grid of polygonal regions where sources with specific properties (stars, circumstellar envelopes with varying degrees of optical thickness, planetary nebulae and other infrared sources) were expected to be found. As is common in these cases, the boundaries between the regions were defined arbitrarily by using a convenient geometrical pattern bisecting known “template” sources used for building the diagrams. Most importantly, these regions did not have an associated statistical meaning, e.g. it was not possible to quantify how complete and effective was the source classification provided by these regions.

Other branches of science, however, have developed statistically valid techniques to attack this kind of unstructured classification problems, where detailed knowledge of a model is not required, or not available. The k-Nearest Neighbors (k -NN) method (Fix & Hodges 1951), in particular, has been successfully used as an efficient “black box” predictor for problems of pattern recognition and unsupervised machine learning, in fields ranging from computerized handwriting recognition (Simard et al. 1993) to automatic classification of satellite imagery (Michie, Spiegelhalter & Taylor 1994), to medical imaging and diagnostics.

In astronomy, k-Nearest Neighbors methods have been traditionally used to study clustering in the spatial distribution of astronomical sources (see e.g. Bahcall & Soneira 1981), by analyzing the statistical distribution of the distances, on the plane of the sky or in the 3-dimensional space, between each source and its nearest neighbors. Alternatively, the method has been the base of regression techniques for parameter fitting (e.g. photometric redshifts, see Ball et al. 2007). In this paper, we will instead apply the k -NN method in its role of nonparametric classifier, where the

class of a new set of data is decided based on its *distance* from a class of “templates”, and where the distance is defined in a multi-dimensional color and magnitude space. Our implementation of the method is specifically tuned to the search of rare sources hidden in a large catalog.

To illustrate the effectiveness of the method, we apply our technique to the search of brown dwarfs with the InfraRed Array Camera (IRAC, Fazio et al. 2004) onboard the *Spitzer* Space Telescope (Werner et al. 2004). As shown by Patten et al. (2006), brown dwarfs have unique colors in the near-IR and IRAC 3.6, 4.5, 5.8 and 8.0 μm bands, due to the presence of prominent molecular features such as CH_4 , H_2O , NH_3 and CO (Oppenheimer et al. 1998; Cushing et al. 2005; Roelling et al. 2004) in the wavelength range covered by the camera (see Figure 1). These colors provide a powerful discriminant to identify brown dwarfs within the large photometric catalogs that have been produced during the *Spitzer* cryogenic mission. The k -NN method is particularly suited for this search, because of its high efficiency in finding “needles in the haystack” such as brown dwarfs, among the galactic general population and the extragalactic background.

The method is first applied using data from the *Spitzer* Extragalactic First Look Survey (XFLS, Lacy et al. 2005) and the *Spitzer* Shallow Survey (Eisenhardt et al. 2004), which are combined with ground based optical and near-IR surveys for further refinement of the candidate sample. The parameter space of the possible color combinations and k -NN parameters is explored in order to provide and quantify the best possible search completeness and efficiency. Searches using only the two IRAC bands at 3.6 and 4.5 μm are also investigated, to assess the possibility of brown dwarf detection using only the two channels that will be available during the post-cryogenic *Spitzer* warm mission.

Section 2 of the paper describes our implementation of the k -NN method, which is then applied in Section 3 to search for field brown dwarfs in the XFLS and Shallow surveys. In Section 4 the k -NN method is used to estimate the efficiency and completeness of IRAC photometric searches of brown dwarf companions around nearby stars. In Section 5 we summarize the results of these searches, and discuss other possible applications of the method.

2. The k -NN Method

In a typical application of the k -NN method, as described by Hechenbichler & Schliep (2004), the class of a test element is selected by a majority vote of its k nearest templates (where k is optimized to the specific problem at hand). Template objects for each class, (i.e the *training sample*) are distributed in the multi-dimensional space defined by the variables used in the analysis. The class of the test element is determined by the prevalent class of the k templates that, according to a given *metric*, are closer to the test element. Note that in this case the choice of the metric is only important for the selection of the k nearest templates, after which the decision is determined by the rule adopted to weight the “votes” of these k nearest templates.

The situation is however different in the classical astronomical setting, where sources of one

specific class are searched among a larger set belonging to many other classes, which are generally not specified. In this case, a majority vote is not possible and a different approach is required. In order to address this challenge, we have developed a novel implementation of the k -NN method tuned for the search of rare sources in astronomical photometric catalogs. Our application requires templates only for the “search class”, relying on the assumption that the templates are an accurate representation of the class, and that the selection variables (colors and magnitudes) chosen in the analysis are sufficient to provide an effective discrimination. The only quantitative criterion available for the selection, and used to determine its statistical validity, will be the final k -NN distance of each source in the input catalog, according to the chosen method. As an example, in section 3 we show the application of our method to the search of brown dwarfs (the *signal*) in a catalog where most of the other sources are galaxies or regular stars in different evolutionary stages (the *background*).

2.1. The k -NN Metric

In any k -NN application the choice of the metric is arbitrary, and is ultimately determined only on the basis of its ability to effectively separate the signal from the background. If the analysis involves N separate variables (in this case colors or absolute magnitudes), a common choice is the euclidean distance in the N th-dimensional space, with the individual distances in each variable averaged (or summed) on the number of dimensions:

$$D(i, j) = \begin{cases} \sqrt{\sum_{l=1}^N d_l(i, j)^2} & \text{euclidean distance} \\ \sqrt{\sum_{l=1}^N \frac{d_l(i, j)^2}{N}} & \text{averaged euclidean distance} \end{cases} \quad (1)$$

where $d(i, j)$ is the distance between the source i and the template j with respect to the variable l . The effect of averaging over the dimensionality N is illustrated in Figure 2: the average increases the size of the ellipse enclosing test sources within a given distance from each template. If a source has a unitary distance from a template along each variable, the distance will be larger than one in the case of a pure euclidean metric, but still equal to one in the case of averaged euclidean metric. The latter is preferable for multi-dimensional spaces where is not desirable to have a metric that tends to become larger as the dimensionality N increases: in other words, it is a good choice to have a distance close to unity if the individual components of such distance in each variable are all around unity. For this reason we have adopted the averaged euclidean distance in this implementation of the k -NN method. Furthermore, another advantage of averaging is that it allows to weight differently the individual components of the metric, in case some of the variables (colors or magnitudes) have a stronger discriminatory property for the problem at hand. However, in the applications presented here we assume for simplicity that all the variables are equally important, and no weighting is necessary.

To ensure that the distances along each variable play an equal role in the final metric, a normalization is required. The metric should take into account, for example, if one color or magnitude has larger uncertainty than the others. Thus we divide each distance by its associated total uncertainty:

$$d_l(i, j) = \frac{x_l(i) - x_l(j)}{\sigma_l(i, j)} \quad ; \quad \sigma_l(i, j) = \sqrt{(\sigma_i^2 + \sigma_j^2)} + \sigma_s(j) \quad (2)$$

where σ_i and σ_j are the statistical uncertainties of the data and templates respectively (e.g. their 3σ photometric error) in the variable l , and where σ_s is a measure of the non-Gaussian systematic errors of the template j (explained below), also in the variable l .

The final k -NN distance of a source i is then the (weighted) average of the distances to the nearest k templates (the optimal number of neighbors k is determined with the techniques described in Section 2.2):

$$D_{kNN}(i) = \frac{\sum_{j=1}^k D(i, j) \cdot w(i, j)}{\sum_{j=1}^k w(i, j)} \quad (3)$$

The weights $w(i, j)$ are introduced to reduce the influence of isolated templates that happen to be much farther away than the other nearest neighbors. A Gaussian kernel is very effective for this task:

$$w(i, j) = \exp \left[\frac{-D(i, j)}{k \cdot \sqrt{\sum_{l=1}^N \sigma_l(i, j)^2}} \right]^2 \quad (4)$$

Note that the Gaussian kernel is parametrized with the geometric average (on all variables l) of the same normalization factor $\sigma(i, j)$ adopted for the individual distances. This is again necessary to scale the range of the kernel proportionally to the accuracy of the individual templates. The extra factor k plays the role of reducing the effectiveness of the kernel as the number of neighbors increases, which is the intended goal of using a large value for k .

The effect of this normalization on the k -NN distance is shown in Figure 3. The contours traced around the template sources enclose the areas within a given k -NN distance from the training sample. The meaning of this region becomes obvious in the case of $k = 1$ (solid line). Thanks to the normalization with the total uncertainty $\sigma(i, j)$, the region with a radius $D_{kNN} = 1$ is nothing else than the union of the error ellipses around the templates. A test source within the region will have a separation from the template class which is less than the uncertainty in the data and the templates, and will thus likely be a member of the template class. A source with $D_{kNN} \gtrsim 1$ will instead have a greater probability of not being a member, and should be rejected. Note that for $k = 1$ the border of the region closely follows the location of the templates, deviating from a smooth line because of the scatter in the distribution of the training sample. A larger value of k , on

the other end, will average on the position of the individual templates, thus producing a smoother contour, albeit at the risk of excluding isolated templates from the region. The best value of k will be a compromise between these two different tendencies, and needs to be determined case by case, with the parameter optimization techniques explained in the following section.

The solid line in Figure 3 was derived without adding the non-Gaussian systematic error σ_s in the templates. As a result, for any given k -NN distance, the size of the region is determined only by the statistical errors in data and templates. A direct consequence of this, however, is that templates that are separated by a distance larger than their statistical error will produce separated regions. This is not desirable, as in most astronomical applications the location of the templates is only partially in control of the astronomer. Due to low statistics it depends on the chance location, in the color-color and color-magnitude space, of the template sources that have been possible to observe. This is particularly true for the search of rare sources, where only a small number of templates is generally available. The sparseness of the templates in this case may lead to a serious problem, as regions of the color-magnitude space where sources of the template class may exist could be excluded only because no templates have been observed there at the time the training sample was assembled. To correct this issue we introduce in our k -NN metric the *sparseness factor* σ_s , which is a measure of how far apart the templates are with respect to each variable l :

$$\sigma_s(j) = \frac{1}{k} \cdot \sqrt{\sum_{t=1}^k d_l(t, j)^2} \quad (5)$$

where $\sigma_s(j)$ is defined as the average distance of the template j from the remaining k nearest templates. The dotted line (for $k = 1$) in Figure 3 shows how the introduction of the sparseness factor σ_s , acknowledging the inadequacy of the template distribution in a region of the parameter space, is able to reconnect the region despite the lack of templates between the two sets that are separated in the solid line region. Particular caution, however, should be taken while introducing the $\sigma_s(j)$ defined as in equation 5 in cases where a gap in the templates distribution is actually expected in the data (e.g. the gap in the Horizontal Branch for He burning giants in the Hertzsprung-Russell diagram). In such cases, the presence of the gap can only be noticed, and is statistically significant, when it is sampled by a large number of templates on both sides of the gap. If k is chosen to be much smaller than the number of templates in the gap region, the gap will still be preserved as no template across the gap will be among the k nearest neighbors in equation 5, and the sparseness factor will be smaller than the width of the gap.

2.2. Application of the Method

The k -NN metric we have defined in Eq. 3 is ideally suited for selecting rare astronomical sources based on their spectral properties from a large photometric catalog.

The first step in applying the method is the identification of the variables to use. These variables can be any combination of colors or magnitudes. Unless the number of available bands is so small that all the possible combinations can be tested, the best course of action is to choose the variables that, based on astrophysical considerations, provide the best discrimination (e.g. colors sensitive to peculiar spectral features). Caution must be used to avoid choosing too many variables: even though one would naively assume that more variables would produce a better selection, this is not always the case and can lead to the so-called “curse of dimensionality” (see e.g. Hastie et al. 2003). Also variables that do not carry a significant discriminating role should be avoided, because they would dilute the effectiveness of the metric by averaging out more effective variables. Having multiple variables sensitive to the same physical property can also be counter-productive, as it biases the metric towards this one physical characteristic, at the expense of other equally or more important discriminants. A solution to this issue is to either to avoid adding variables not contributing any original discriminant, or to reduce their influence by fine-tuning the k -NN metric with appropriate weights.

Once the variables are chosen, the D_{kNN} distance of each source in the catalog can be determined. The selection is done by comparing D_{kNN} with a threshold value D_{th} above which the sources are rejected. For maximum effectiveness the number of neighbors k and the threshold distance D_{th} have to be optimized for the problem at hand. The goal of this optimization is to select the smallest possible number of candidates to follow-up, while preserving the completeness of the search. In this context, we define the *completeness* \mathcal{C} as the fraction of the objects that are found, with respect to their expected number. In addition, we define the *rejection efficiency* \mathcal{E} as the fraction of the background objects that are successfully rejected. An ideal search will have 100% completeness (all sources are found) and 100% rejection efficiency (all the returned candidates are genuine). In practice both fractions will be lower than 1, and the search parameters should be optimized to provide maximum possible rejection efficiency and completeness. This optimization can be done using either the *jackknife* or the *bootstrap* methods (Hastie et al. 2003). Both methods attempt to estimate the statistical distribution of $\mathcal{C}(k, D_{th})$ and $\mathcal{E}(k, D_{th})$ to determine the best values of k and D_{th} .

The jackknife method tests the minimum distance for which the templates are an homogeneous and contiguous set. Given a certain k , one measures the k -NN distance of each template from the remaining $n - 1$ (leave-one-out method). Once this is done for all templates, the completeness is derived as the fraction of templates that are within any given threshold distance D_{th} . While this method is relatively straightforward, it may be very inaccurate for the search of rare sources, since the number of available templates is often small and does not cover uniformly the color and magnitude distribution of the target objects. Thus we adopt the bootstrap method.

With the bootstrap method we evaluate the completeness by creating an artificial sample with the characteristics of the templates. This artificial sample is then tested with the k -NN method to estimate how many of these simulated sources are found within a distance D_{th} . The test sample is generated by varying the template colors and magnitudes, adding a random offset

using the statistical and systematic errors in the templates. The statistical errors are introduced by adding a Gaussian error equal to the statistical uncertainty of the templates (σ_j in equation 2). The systematic errors are instead simulated by adding a random uniform component equal to the amplitude of the template sparseness factor σ_s defined in equation 5. With this method it is possible to create an arbitrary number of simulated signal and background samples of any size, enabling the study of the statistical distribution of $\mathcal{C}(k, D_{th})$ even when only a small number of templates is available.

The rejection efficiency \mathcal{E} is similarly evaluated with the bootstrap method. If a “pure” background sample can be extracted from the catalog, then it is just a matter of counting the fraction of catalog sources that are rejected with any combination of k and D_{th} . In most cases a pure background sample is however not available but, if the objects in the search class are rare, any small sub-sample of the full catalog can be assumed to have a very small contamination of template-class sources. These sub-samples can be randomized introducing Gaussian noise equal to the data uncertainty σ_i defined in equation 2. Sub-samples that by chance have a larger level of contamination will appear as outliers, and can be removed from the final distribution of $\mathcal{E}(k, D_{th})$.

Once the distribution of \mathcal{C} and \mathcal{E} is known, the characteristics of the selection problem determine the value of k and D_{th} to choose. If the search needs to be very selective because a large number of follow-up observations is not affordable, then the completeness can be sacrificed (generally by using a small value of D_{th}) in favor of high \mathcal{E} . On the contrary, when completeness is paramount, a larger threshold distance can be adopted even though it will result in a large number of candidates. As an intermediate solution we adopt the value of D_{th} and k for which $\mathcal{E}(k, D_{th}) = \mathcal{C}(k, D_{th})$ is the highest.

After the k -NN metric is applied with the optimized parameters, all sources within the threshold distance D_{th} should be considered as candidates. These candidate sources can be followed-up by applying further selection criteria (e.g. applying color cuts that could not be included in the k -NN metric, or by executing new targeted observations). If the selected sample is still too big for a follow-up program, it can be helpful to run the k -NN method a second time on the first-run selection, using a different set of variables. This is particularly effective if there is a concern that some variables have yielded a lower selection efficiency than expected, due to having been averaged out in the metric by other variables. In this case it may be just more efficient to re-apply the k -NN method using only these variables, starting from the sources selected in the first run, rather than trying to improve the efficiency of the first k -NN run by fine tuning the weights between the variables.

3. Searching Brown Dwarfs in *Spitzer* Wide Field Surveys

As an application of the method, we present the search of brown dwarfs in *Spitzer* surveys. Brown dwarfs represent the link between main sequence stars, fully supported by H burning in their

cores, and planets. Given our poor understanding of the lower end in the stellar mass distribution, an accurate census of the galactic population of brown dwarfs is of paramount importance to constrain models of star formation and galactic evolution, and to provide an accurate measurement of the stellar mass in the Galaxy.

Due to their low luminosity and red colors, brown dwarfs are difficult to find. The first unambiguous identification of a brown dwarf, Gliese 229B (Oppenheimer et al. 1995), came only 20 years after the class was introduced by Jill Tarter in her Ph.D. thesis. In recent years, however, the availability of deep wide area surveys such as the Two Micron All Sky Survey (2MASS, Skrutskie et al. 2006), the Deep Near Infrared Survey of the Southern Sky (DENIS, Epchtein et al. 1999), the Sloan Digital Sky Survey (SDSS, York et al. 2000) and the UKIRT (UK Infrared Telescope) Infrared Deep Sky Survey (UKIDSS, Lawrence et al. 2007) allowed to identify an increasing number of brown dwarfs in the solar neighborhood (see e.g. Kirkpatrick et al. 2000; Burgasser et al. 2002; Leggett et al. 2002; Geballe et al. 2002; Burgasser 2004; Knapp et al. 2004; Tinney et al. 2005; Chiu et al. 2006; Cruz et al. 2007;Looper et al. 2007; Pinfield et al. 2008). However, the total number of brown dwarfs known to date (~ 556 of the red, dusty L dwarfs, and ~ 148 of the cooler, methane rich T dwarfs, according to the DwarfArchives.org database) is still too small to provide a reliable characterization of the substellar mass function.

The sensitivity of the IRAC instrument onboard *Spitzer*, and the characteristics of its photometric system, raised expectations for a large increase in the number of brown dwarfs (especially the cooler T dwarfs) detected using wide area *Spitzer* surveys. These expectations, however, have not yet materialized. Only three T dwarfs have been discovered by *Spitzer*: a T4.5 field dwarf in the Extragalactic *Spitzer* Shallow Survey (Stern et al. 2007), and two T dwarf companions around the nearby young stars HN Peg and HD 3651 (Luhman et al. 2007). This state of affairs arises from the complexity of discriminating brown dwarf candidates from the large number of extragalactic red sources that are within the detection limits of IRAC observations.

The success of photometric searches ultimately depends on the efficiency of the selection method required to extract from these large catalogs a manageable sample of sources for spectroscopic follow-up. This selection is usually done by applying cuts in the color and magnitude space (see e.g. Cruz et al. 2003 and Burgasser et al. 2003 and references therein). Stern et al. (2007), in particular, used a single IRAC color cut, $[3.6] - [4.5] \geq 0.4$, to select T dwarfs with deep CH₄ absorption in the 3.6 μm IRAC band, complemented by criteria based on the photometry and the morphology of the sources in optical bands. These criteria are not able to discriminate between brown dwarfs and high redshift quasars, and are limited to the detection of dwarfs of spectral type T3 to T6. The *k*-NN method proposed here has been designed to analyze datasets in a multi-dimensional color and magnitude space, based only on the distribution of templates without the need to define a-priori cuts. Thus it is in principle capable to go beyond these limitations, opening the search to L and early-T dwarfs and T dwarfs of type later than T6, without introducing the biases associated with the choice of the cuts, and provide a more efficient and complete search. This will be especially important during the *Spitzer* Warm Mission planned from the spring of

2009 when, upon exhaustion of the cryogenic LHe, the observatory will be tasked to conduct large area surveys using only the IRAC bands at 3.6 and 4.5 μm (Storrie-Lombardi & Silbermann 2007).

In this section we study how to improve on the selection efficiency of *Spitzer*/IRAC search of brown dwarfs using the k -NN method. We explore the k -NN parameter space to understand the best strategy for these searches, and what are the requirements, in terms of auxiliary data, for their success. We also develop techniques that allow to assess the completeness of the result, necessary to draw statistically valid conclusions from these searches.

3.1. Sample Selection

As test datasets to illustrate our k -NN search for brown dwarfs, we use two publicly available *Spitzer*/IRAC wide field surveys: the XFLS (Lacy et al. 2005) and the Boötes field of the IRAC Shallow Survey (Eisenhardt et al. 2004).

The XFLS main field covers an area of 3.8 deg² at high galactic latitude, observed to a sensitivity reaching a 5σ Vega magnitude of 18.9, 18.0, 15.7 and 15.1 at 3.6, 4.5, 5.8 and 8.0 μm respectively (obtained with integration times of at least 60 sec per pointing). The XFLS main field was chosen for the availability of extensive auxiliary data, including SDSS and 2MASS. The Boötes field of the Shallow Survey instead covers an area of 8 deg² with limiting 5σ Vega magnitudes of 18.4, 17.7, 15.5 and 14.8 at 3.6, 4.5, 5.8 and 8.0 μm respectively (integration time ≥ 90 sec). Deep near-IR J and K_s data has been obtained as part of the FLAMINGO Extragalactic Survey (FLAMEX, Elston et al. 2006) for 7.1 deg² of the IRAC field, and in the optical as part of the NOAO Deep Wide-Field Survey (NDWFS, Jannuzi & Dey 1999).

The main difference between the two samples (apart for the Shallow Survey being almost twice the area of the XFLS), is in the depth of the optical and near-IR ancillary data. While SDSS provides 5σ detection limits of 22.3, 23.3, 23.1, 22.3 and 20.8 in u' , g' , r' , i' and z' (York et al. 2000), NDWFS has 5σ point source depths of 27.1, 26.1 and 25.4 in B_W , R and I respectively (Stern et al. 2007). 2MASS provides 5σ sensitivity in J , H and K_s of 16.6, 15.9 and 15.1 respectively (Skrutskie et al. 2006), while FLAMEX approaches a 5σ sensitivity of 21.4 and 19.5 in J and K_s (Elston et al. 2006). The added depth of the NDWFS and FLAMEX data provides a powerful tool to resolve ambiguities between red sources in the IRAC bands of galactic and extragalactic nature. By testing our method on both datasets we can measure the efficiency of the brown dwarf search on surveys with different depth and assess the auxiliary data requirements necessary to enable effective brown dwarf searches during the *Spitzer* warm mission.

Figure 4 shows the distribution of point sources from the XFLS in a number of IRAC and 2MASS colors, compared with the distribution of 37 L, 7 early-T ($T < 4.5$) and 22 late-T ($T > 4.5$) templates from Patten et al. (2006). We chose the colors in the diagrams to maximize the separation between brown dwarfs and other galactic (clump near zero colors) and extragalactic (long plume with red colors) sources. In particular (see Figure 1): (1) the $J - [3.6]$ color is effective in separating

the L dwarfs from regular stars, mainly due to H₂O absorption in the J band; (2) the $K_s - [4.5]$ and $[3.6] - [4.5]$ colors separate the T dwarfs from all other sources (L dwarfs, regular stars and extragalactic objects), due to the increasing CH₄ absorption in the K and 3.6 μm bands; (3) the $[4.5] - [5.8]$ color is useful to select again the T dwarfs, which appear blue because of H₂O absorption in the 5.8 μm band; and (4) the $[3.6] - [8.0]$ color is also providing a strong separation of the T dwarfs due to the methane absorption which is stronger at shorter wavelength than in the reddest IRAC band. Color combinations using the H band have a similar discriminatory power than colors with the J and K_s photometry: $H - [3.6]$ shows a trend analogous to the $J - [3.6]$ color, and $H - [4.5]$ has a very similar color trend than $K_s - [4.5]$. The $J - K_s$ colors provide a similar discrimination than the $[3.6] - [4.5]$ colors, because of CH₄ absorption stronger in the K_s than the J band.

The late-T dwarfs appear well separated from any other source, thanks especially to the $[3.6] - [4.5]$ IRAC color, even though some contamination persists with red high-redshift quasars having PAH emission. The early-T and L dwarfs are however more difficult to discriminate because, once dispersion due to photometric errors is taken into account, their color space is very similar to the one occupied by low-redshift galaxies and regular stars. For this reason, and due to the relative small number of early-T dwarfs in the Patten et al. (2006) sample, our k -NN selection is done for two separate classes only: one comprising all L and early-T templates, and one with late-T (with $T > 4.5$) dwarfs.

To explore the effect of the presence or absence of individual bands in the selection efficiency, we have divided our XFLS and Shallow Survey catalogs in 2 different subsamples: (1) sources having 3σ photometry in J , K_s and all four IRAC bands; (2) sources having 3σ detection in J , K_s , 3.6 and 4.5 μm . The first sample is intended to test the effectiveness of the k -NN method when all IR bands are available (the H band has not been considered because of its unavailability in FLAMEX, and because brown dwarf colors using the H band are very similar to the colors using J and K_s). The second sample is instead designed to simulate the case of the *Spitzer* Warm Mission, when only the two short wavelength IRAC channels will be available, and also to avoid the limitations imposed by the less sensitive 5.8 and 8.0 μm bands in currently available surveys. For each sample the search is done using a subset of the available colors, avoiding the repetition of similar colors, that would dilute the k -NN metric. The characteristic of the individual subsamples, their size and the color combinations used in the k -NN search are listed in Table 1. Optical photometry and imaging are not used at this stage, because only a limited number of the brown dwarfs we are using as templates have reliable magnitudes at optical wavelengths. The optical data will however be crucial to refine the search results later on.

3.2. Parameter Optimization

The best values of k and D_{th} for the search can be determined by using the bootstrap method described in section 2.2. The goal is to optimize the k -NN parameters in order to have the smallest

possible number of candidates that will need follow-up observations while preserving the completeness of the search. The jackknife method is not suitable in this case because of the very small number of available templates in each brown dwarf class.

The completeness of the search in this case is $\mathcal{C} = 1 - n_{FN}/n_{exp}$, where n_{exp} is the number of brown dwarfs expected to exist in the dataset and n_{FN} is the number of false negatives (i.e. true brown dwarfs not identified) in the search. The rejection efficiency can be written as $\mathcal{E} = 1 - n_{FP}/n_{tot}$ where n_{FP}/n_{tot} is the fraction of false positives, i.e. the number n_{FP} of incorrectly identified brown dwarfs, with respect to the total number of sources n_{tot} in the sample.

Figure 5 shows the rejection efficiency and completeness for a Monte Carlo test using 100 randomized samples each with 500 background sources and 500 simulated brown dwarfs, for $k = 3, 5$ and 7 . The simulations are made for the subsample using IRAC plus J and K_s bands (for both L/early-T and late-T searches), and for *Spitzer* warm mission colors (as described in Table 1). The figure shows the resulting rejection efficiency and completeness for the XFLS; similar results are obtained for the Shallow Survey.

The rejection efficiency curve is a decreasing function of D_{th} because when sources with larger k -NN distances are selected it is more likely to include false positives in the candidates. On the other hand, for smaller D_{th} more true brown dwarfs are missed, leading to a smaller completeness. We have adopted the D_{th} for which the two curves cross. The values of D_{th} at the \mathcal{E} and \mathcal{C} crossing point for $K = 3, 5$ and 7 are listed in Table 2 for simulations of the XFLS and Shallow Survey search subsamples. Note that D_{th} tends to be smaller for L/early-T than for late-T searches. This is because (as shown in Figure 5) the efficiency \mathcal{E} of L/early-T searches drops faster with D_{th} than in late-T searches, due to the IRAC colors of L/early-T dwarfs being relatively similar to the colors of regular late spectral type stars and low redshift galaxies (see Figure 4): in L/early-T searches even a small increase in D_{th} results in a large contamination of background sources and thus in a fast drop of the efficiency \mathcal{E} . As a result, in L/early-T searches the crossing point $\mathcal{E} = \mathcal{C}$ occurs for smaller values of D_{th} than in late-T searches where, thanks to the unique colors of late-T dwarfs, the efficiency drops slowly as a function of D_{th} .

Table 2 shows that the search of late-T dwarfs using IRAC and near-IR colors combined reaches high level of completeness and rejection efficiency, up to 99.9%. Even if only the two short wavelength IRAC bands are used (as will be the case in the warm mission), \mathcal{E} and \mathcal{C} are still similarly high. Note however that the completeness and rejection efficiency of the warm mission search tend to be smaller when IRAC photometry is combined with the deeper FLAMEX dataset, rather than the shallower 2MASS, due to the higher number of red extragalactic sources cross-correlated with the IRAC catalog. The L/early-T search is less efficient than the late-T search, with \mathcal{C} and $\mathcal{E} \sim 90\%$, due to the higher contamination of this sample with background sources with similar colors.

Rejection efficiency and completeness are generally higher for small k , because in that case the selection region follows more closely the distribution of the templates. Using small k , however,

puts us at risk of depending critically on outliers in the template class. We adopted $k = 5$ for the searches done using all IRAC bands. For the search in “warm mission” condition, however, we adopted $k = 3$ to have the maximum possible efficiency, given the larger size of the initial catalog.

3.3. k -NN Search Result and Optical Validation

The results of the k -NN search for brown dwarfs are presented in Table 3. The table shows, for each subsample of the XFLS and Shallow Survey, the number N_{sel}^{kNN} of selected sources. The actual rejection efficiency $\mathcal{E}' = 1 - N_{sel}^{kNN}/N_{tot}$ (where N_{tot} is the number of sources in each subsample) is also shown. Comparison with Table 2 shows that \mathcal{E}' is very similar to the rejection efficiency \mathcal{E} predicted by the bootstrap method Monte Carlo simulations.

Table 3 shows that, when all IRAC bands are available, the k -NN method alone is efficient enough to reduce the number of possible candidates to a size small enough to allow visual inspection of the candidates. As only the k -NN method is used, the selected candidates are not biased by the choice of arbitrary cuts, depending only on a metric with known completeness, normalized on the statistical uncertainties of both data and templates. Optical data are however available, and can be used to further reduce the candidate sample, which is still necessary in the case of L/early-T dwarf searches, and when requiring only 3.6 and 4.5 μm photometry (resulting in a much larger catalog).

The low temperature of brown dwarfs requires their optical colors to be very red, in contrast with the case of extragalactic objects that tends to have a flatter optical SED. In particular, according to Leggett et al. (2000), L dwarfs have $i' - z' > 1.6$ in the SDSS photometric system, while T dwarfs have $i' - z' > 3.0$. According to Dahn et al. (2002) L and early-T dwarfs have $R - I > 2.0$ while according to Stern et al. (2007) late-T dwarfs must have $R - I > 2.5$ in the NDWFS bands. These criteria can be applied to all selected sources, as long as their i' and z' magnitudes (for sources in the SDSS) or R and I magnitudes (for NDWFS sources) are known. Sources missing optical photometry can still be considered as brown dwarf candidates, given that their absence from the optical catalog may be an indication of very red colors. These colors cannot be introduced directly in the k -NN metric because good photometry in the optical bands is missing for a significant fraction of our templates. By using the optical bands in the form of “cuts” we are introducing a bias associated to the choice of the cut. However this is still more efficient than doing the selection using cuts alone, since the candidates have been pre-selected in an unbiased mode using all the other bands with the k -NN metric. This allows us to adopt a less stringent optical color criteria while still preserving very high efficiency in the selection. It also allows to retain the candidates selected with the k -NN method that are missing optical data (the potentially coolest late-T candidates), which would be eliminated by default if color cuts were the only selection criteria.

The application of the criteria described above reduces drastically the number of viable candi-

dates. The remaining candidates can then be checked visually from the SDSS and NDWFS plates, to eliminate all sources that appear extended, that are blended with other sources, or that are corrupted by artifacts in the images. The remaining candidates are listed in Table 4 and 5. The number of viable candidates after the optical criteria are applied is listed in Table 3, separately for the N_{sel}^{opt} sources that possess optical detection, and the $N_{sel}^{no\ opt}$ that are not detected in the optical surveys.

Note that when all IRAC, J and K_s photometry is known, cross-checking with optical data reduces the number of late-T dwarf candidates to zero for the XFLS, and to only one for the Shallow Survey. The lone T dwarf selected for the Shallow Survey is in fact the T4.5 dwarf IRAC J142950.8+333011 found by Stern et al. (2007) in their search. This result shows that the k -NN method, when used on near-IR and *Spitzer* data, in combination with deep optical photometry is capable to select true late-T dwarfs while rejecting all other sources of different nature. In fact, the method here described effectively rejected the second red source found by Stern et al. 2007 color cuts, the $z = 6.12$ radio-loud quasar IRAC J142738.5+331242.

Figure 6 shows the $K_s - [4.5]$ and $[3.6] - [4.5]$ colors of all the candidates selected in both surveys. Of the plotted sources, 5 have colors at odd with the brown dwarf templates. These sources, most likely red background galaxies, have identical colors than T dwarfs in all bands, with the exception of the two plotted here. The fact that they have been selected by the k -NN method is an example of “variable dilution” in the metric, as described in section 2.2. To refine the selection we can apply a second time the k -NN method, using only this pair of variables, the $K - [4.5]$ and $[3.6] - [4.5]$ colors. The region corresponding to $k = 3$ and $D_{th} = 0.8$ (providing completeness $\mathcal{C} \gtrsim 99.9\%$ in these two variables) is plotted in Figure 6, and confirms that these sources are outliers. We flagged them as such in Table 5.

After these anomalies are taken into account, we are left with 1 viable L/early-T and no viable late-T candidates in the XFLS (Table 4), and 3 viable L/early-T candidates and 1 late-T dwarf (the T4.5 dwarf J142950.5+333011) in the Shallow Survey (Table 5). The L/early-T viable candidates need follow-up observations (currently in progress) to determine unambiguously their nature.

4. Searching Low Mass Companions around Nearby Stars

As a second example illustrating the case of k -NN metric using not only colors but also absolute magnitudes, we show the case of the search of low mass companions around nearby stars. This search was conducted as part of the IRAC Guaranteed Time Observations (P.I. Giovanni Fazio) programs PID 33, 34, 35, 36, and 48 (Patten et al. 2005). The survey focused on 400 stars within 30 pc from the Sun, among which all stars and brown dwarfs within 5 pc known to date. The sample included young stars with age ≤ 120 Myr, stars with known radial velocity discovered exoplanets, and the L and T dwarfs from Patten et al. (2006) used here as templates. Each star was imaged to a depth of of ~ 150 sec in all IRAC bands, with a field of view of ~ 5 arcmin, sufficient to detect

companions at a distance of ~ 50 to 4,000 AU from the primary, to a limiting mass of $\sim 10\text{--}20 M_J$. The search has yielded the discovery of two new T dwarfs from the whole sample, presented in Luhman et al. (2007). All the observations were made in a single epoch, preventing the search of companions by virtue of their common proper motion with the primary (except for the few cases in which a deep near-IR image was available). The candidate selection was instead based on the k -NN method described below. While a paper analyzing the search results is in preparation (Carson et al., 2009), we want here to discuss the efficiency of the k -NN method in this particular case of brown dwarf search.

Figure 7 shows simulated $[4.5]$ vs. $[3.6] - [4.5]$ photometry of L, early-T and late-T dwarfs around a nearby star at 5, 10 and 20 pc. To simulate the photometry of background sources around the primary star, we have used the XFLS catalog, which is an adequate representation of a background field projected at high galactic latitude. For nearby stars projected closer to the plane of the Galaxy, the proportion of extragalactic/galactic sources will be smaller, reducing the contamination from red extragalactic sources, while contamination from red galactic sources is likely to be increased. The latter (mass losing evolved stars and young stellar objects) may however be discriminated by means of auxiliary infrared observations capable of detecting the thermal emission from their circumstellar dust. Figure 7 also shows k -NN regions plotted for $k = 5$ and $D_{th} = 1$. By adding the $[4.5]$ magnitude to the k -NN variables the selection is in principle improved because a large fraction of the red background extragalactic sources are fainter than the expected brightness of brown dwarf companions. This is especially true for T dwarfs around stars within 5–10 pc from the Sun. This advantage is reduced for searches around farther stars, since the brightness of T dwarf companions at $d \simeq 20$ pc is the same of the extragalactic background.

We have estimated the rejection efficiency and completeness of this search using the same bootstrap method described in section 2.2. Table 6 shows that for early-T dwarfs the selection efficiency reaches very high values (up to 99% for primaries at 5 pc). For late-T dwarfs the rejection efficiency is approximately the same that is obtained by using only colors as selection criteria, and the inclusion of absolute magnitudes does not result in a dramatic improvement in the search effectiveness (suggesting that the k -NN color selection is already close to maximum efficiency). The \mathcal{E} and \mathcal{C} obtained in the simulations, are adequate for this kind of search: the typical number of sources in the ~ 400 stars part of the IRAC companion search program had an average of ~ 100 background sources each. With this efficiency, for each field the chosen k -NN criteria selected up to 3 candidates, many of them actually present in at least one 2MASS map, and could be ruled out either by the absence of proper motion, or because they did not possess the correct near-IR colors. The few remaining candidates were followed-up spectroscopically and by acquiring deep near-IR images, resulting in the two new T dwarfs found around HN Peg and HD 3651, presented in Luhman et al. (2007).

5. Discussion and Conclusions

Based on the photometry given by Patten et al. (2006), the sensitivity of the XFLS and the Shallow survey in the IRAC bands allows for the detection of late-T dwarfs (T4 to T8 spectral type) up to a distance of ~ 20 pc. This limit is determined mainly by the lower sensitivity of the 5.8 and 8.0 μm bands, for the latest spectral types. If only the 3.6 and 4.5 μm bands are used, as in the *Spitzer* warm mission, the higher sensitivity allows detection of late-T dwarfs up to a distance of ~ 50 pc. The detection limit at the L-T boundary is ~ 60 pc (~ 140 pc if only the 3.6 and 4.5 μm bands are required). Within this volume (corrected for the Malmquist bias), we can expect a brown dwarf search to be as complete as $\mathcal{C} \gtrsim 98\%$, as estimated in section 3.2 (multiplied by the completeness of the original survey, and corrected for binarity).

Searches using 2MASS photometry, however, will have more stringent limits, of $\lesssim 5$ pc for late-T dwarfs and ~ 25 pc at the L-T boundary. The sensitivity of the FLAMEX survey is such that any L or T dwarf detected in the IRAC 3.6 and 4.5 μm bands will also be detected in the *J* band, even though the lower sensitivity of the *K* band limits the maximum detection distance for a T8 dwarf to ~ 32 pc. The very small number of brown dwarf candidates that are not optically detected in at least the *I* band shows that the depth of the NDWFS is not a significant constraint in the search of brown dwarfs. The main limitation rather comes from the depth of the IRAC data.

These considerations come into play to understand the potential for brown dwarf searches in the recently approved Exploration Science surveys in the *Spitzer* warm mission. The requirements for brown dwarf detection are clearly a large survey area, deep observations and the availability of matching near-IR and possibly optical data. Of the approved warm mission programs, three satisfy these requirements: the “*Spitzer* Extragalactic Representative Volume Survey (SERVS)” (PI Mark Lacy, PID 60024), the “*Spitzer* Extended Deep Survey (SEDS)” (PI Giovanni Fazio, PID 60022) and the “GLIMPSE360: Completing the *Spitzer* Galactic Plane Survey” (PI Barbara Whitney, PID 60020).

Our analysis shows that when near-IR data of sufficient depth are available (as in the case of the FLAMEX survey), the search for late-T dwarfs using the photometric *k*-NN technique described in section 3 is extremely efficient and complete (more than 99.8% \mathcal{E} and \mathcal{C}). Once a single *I* – *R* or *i'* – *z'* optical color is applied, the final selection produces a very small number of viable candidates to be checked individually (4 L/early-T and 1 late-T viable candidates). It is worth noting that the only late-T dwarf candidate selected in our search is indeed a T4.5 dwarf, as discovered by Stern et al. (2007). With $\mathcal{C} \simeq 98\%$ completeness we can assert that this is the only late-T dwarf present in the volume of the survey (7.1 deg^2 for the FLAMEX field with a depth of ~ 32 pc), even when only the two short wavelength IRAC bands are considered. This number is consistent with the results from the T dwarf UKIDSS DR2 Large Area Survey (Pinfield et al. 2008), that estimates 17 ± 4 late-T dwarfs in an area of 280 deg^2 for a depth of $K \simeq 18.2$ (corresponding to a maximum distance of ~ 18 pc for T8 dwarfs). By factorizing the search volume between the

two surveys¹ one predicts ~ 2 – 3 late-T dwarfs in the volume of the Shallow Survey analyzed in this paper. This is consistent with our result (1 viable candidate in the FLAMEX search), upon considering Poisson statistics. The number of L/early-T candidates that we found shows that, with $\mathcal{C} \sim 85\%$ completeness, ≤ 3 L/early-T dwarfs are present in the Shallow Survey searchable volume ($8 \text{ deg}^2 \times 60 \text{ pc}$).

These numbers can be used to estimate the potential yield of brown dwarfs in the approved warm *Spitzer* Exploration Science surveys. The most promising *Spitzer* warm mission project for the application of the k -NN method here described is the SERVS survey. With a total area of 18 deg^2 , and a total exposure time of 600 sec per pointing, it will probe a brown dwarf volume almost 9 times larger than the IRAC Shallow Survey (search depth of $\sim 80 \text{ pc}$ for late-T dwarfs²). A large fraction of the survey will overlap with the VIDEO VISTA survey³, providing a depth of 25.7, 24.6, 24.5, 24.0 and 23.5 mags in the z , Y , J , H and K bands, more than matching the depth of SERVS in the IRAC 3.6 and $4.5 \mu\text{m}$ bands. Based on these sensitivity, SERVS may find as many as ~ 27 late-T dwarfs and a large number of L and early-T dwarfs.

The SEDS program, on the other hand, has a much smaller survey area ($\sim 0.9 \text{ deg}^2$) but a much longer integration time (12 hours per pointing). This scales down to a searchable volume of ~ 12 times the total volume of the Shallow Survey (search depth of $\sim 230 \text{ pc}$ for late-T dwarfs). This survey can potentially provide as many as ~ 36 late-T dwarfs, even though a decrease in the brown dwarf density should be expected as the survey probes farther distances from the galactic mid-plane. This survey, however, may be limited by the challenge of finding ancillary optical and near-IR data matching the depth of the IRAC photometry. While this may limit the effective late-T dwarf searchable volume, the potential search depth offered by the IRAC data, in a high galactic latitude region, will provide an important test for the vertical distribution of the brown dwarf population in the Galaxy.

The GLIMPSE360 survey, instead, compensates the rather shallow coverage (36 sec integration time for each pointing) with a very large survey area (187 deg^2). A substantial portion of this area is also covered by the UKIDSS survey (Lawrence et al. 2007), implying that ~ 11 of the 17 late-T dwarfs estimated for the whole UKIDSS may be present in the GLIMPSE360 area. According to the GLIMPSE360 consortium, more detailed simulations by Burgasser (2004) predict 70 T0, ~ 100 T5 and ~ 15 – 20 T8 dwarfs in the survey search area. The challenge will be to isolate these brown dwarfs from the high-confusion galactic field, and distinguish them from other red galactic sources. The k -NN method can play an important role for this task.

The main advantage of the k -NN method presented in this paper is that it allows to perform

¹ $V_2/V_1 \propto \Omega_2/\Omega_1 \cdot (d_2/d_1)^3$, where $\Omega_{1,2}$ are the survey areas and $d_{1,2}$ their search distance limit

²Search depth d scales as the limiting flux $F^{1/2}$, in turn scaling as the signal-to-noise ratio $S/N \sim t^{1/2}$, where t is the exposure time. This gives $d \sim t^{1/4}$ and thus $V_2/V_1 \propto \Omega_2/\Omega_1 \cdot (t_2/t_1)^{3/4}$

³<http://www.vista.ac.uk/index.html>

photometric searches using a large number of color and magnitude variables, defining complex regions that closely follow the distribution of the sources to be selected. While similar regions can be defined manually, our method prevents the introduction of biases in the selection due to the choice of the cuts. With the k -NN method the selection regions in the color/magnitude space are only based on the photometric properties of the search class and the statistical uncertainties of the data. Also, the k -NN search can be controlled by just two parameters (the number of neighbors k and the threshold distance D_{th}), instead of many arbitrary cuts, which allows to quickly experiment different combination of variables, and optimize the search for maximum rejection efficiency and completeness.

The examples presented in this paper show that the k -NN method is an effective procedure for the search of field and companion brown dwarfs in *Spitzer* wide field surveys. This can be an important asset for the *Spitzer* warm mission surveys. As these surveys will image areas of the sky where deep photometric catalogs in the optical and near-IR are already available, or in progress, the k -NN method can effectively select T dwarf candidates, potentially leading to a significant increase in the known number of members in this class. This is by no means the only potential application for this method. The method is general enough to allow the photometric selection of sources of any kind, as long as a sample of templates is available. If enough classes of templates are used, the k -NN method can be the engine for the photometric classification of all sources in a survey, by attributing to each source the class with the highest k -NN score. We are currently applying this method of classification to the point source catalog of the SAGE survey (Meixner et al. 2006).

This work is based in part on observations made with the *Spitzer* Space Telescope, which is operated by the Jet Propulsion Laboratory, California Institute of Technology under a contract with NASA. This publication makes use of data products from the Two Micron All Sky Survey, which is a joint project of the University of Massachusetts and the Infrared Processing and Analysis Center/California Institute of Technology, funded by the National Aeronautics and Space Administration and the National Science Foundation. It also used data from the Sloan Digital Sky Survey (see full acknowledgment at <http://www.sdss.org/collaboration/credits.html>), and software provided by the US National Virtual Observatory, which is sponsored by the National Science Foundation. We thank the *Spitzer* Shallow Survey and FLAMINGO Extragalactic Survey (FLAMEX) teams for permission to use data from their surveys. We also thank the National Optical Astronomy Observatory (NOAO) Deep Wide-Field Survey Team for providing the optical and near-IR imaging data used in the Boötes field. NOAO is operated by the Association of Universities for research in Astronomy (AURA), Inc., under a cooperative agreement with the National Science Foundation. The authors would finally like to thank Peter Eisenhardt, Daniel Stern, Mark Brodwin and Buell Jannuzi for useful discussions and suggestions, and the anonymous referee for insightful comments that helped improving this manuscript.

Facilities: Spitzer (IRAC), 2MASS, SDSS, NVO

REFERENCES

- Bahcall, J. N., Soneira, R. M. 1981, *ApJ*, 246, 122
- Ball, N. M., Brunner, R. J., Myers, A. D., Strand, N. E., Stacey, L. Alberts, Tcheng, D. & Llorá, X. 2007, *ApJ* 663, 774
- Burgasser, A. J. et al. 2002, *ApJ*, 564, 421
- Burgasser, A. J., Kirkpatrick, J. D., McEwain, M. W., Cutri, R. C., Burgasser, A. J., Skrutskie, M. F. 2003, *AJ*, 125, 850
- Burgasser, A. J. 2004, *ApJS*, 155, 191
- Burgasser, A. J. et al. 2006, *ApJS*, 166, 585
- Burrows, A., Sudarsky, D., Hubeny, I. 2006, *ApJ*, 640, 1140
- Chiu, K. et al. 2006, *AJ*, 131, 2722
- Cruz, K. L., Reid, I. N., Liebert, J., Kirkpatrick, J. D., Lowrance, P. J. 2003, *ApJ*, 126, 2421
- Cruz, K. L. et al. 2007, *AJ*, 133, 439
- Cushing, M. C., Rayner, J. T. & Vacca, W. D. 2005, *ApJ*, 623, 1115
- Dahn, C. C. 2002, *AJ*, 124, 1170
- Eisenhardt, P. R. et al. 2004, *ApJS*, 639, 816
- Elston, R. et al. 2006, *ApJ*, 639, 816
- Epchtein, N. et al. 1999, *A&A*, 349, 236
- Fazio, G. G. et al. 2004, *ApJS*, 154, 10
- Fix, E., Hodges, J. 1951, Technical Report 21-49-004, 4 US Air Force, School of Aviation Medicine, Randolph Field, TX
- Geballe, T. R. et al. 2002, *ApJ*, 564, 466
- Jannuzi, B. T. & Dey, A. 1999, in *ASP Conf. Ser.* 191, *Photometric Redshifts and High-Redshift Galaxies*, ed. R. Weymann et al. (San Francisco: ASP), 111
- Hastie, T., Tibshirani, R. & Friedman, J. 2003, “The Elements of Statistical Learning”, 2nd Edition, Springer Verlag, ISBN: 978-0-387-95284-0
- Hechenbichler, K., Schliep, K. P. 2004, SFB 386, Discussion Paper 399, Ludwig-Maximilians University, Munich

- Kirkpatrick, J. D. et al. 2000, *AJ*, 120, 447
- Kirkpatrick, J. D. 2005, *ARA&A*, 43, 195
- Knapp, G.R. et al. 2004, *AJ*, 127, 3553
- Macy, M. et al. 2005, *ApJS*, 161, 41
- Lawrence, A. et al. 2007, *MNRAS*, 370, 1599
- Leggett, S. K. et al. 2000, *ApJ*, 536, L35
- Leggett, S. K. et al. 2002, *ApJ*, 564, 452
- IRAS Catalogues and Atlases, Atlas of Low Resolution Spectra, IRAS Science Team 1986, *A&AS*, 65, 607
- Looper, D. L., Kirkpatrick, J. D. & Burgasser, A. J. 2007, *ApJ*, 669, 97
- Luhman, K. L. et al. 2007, *ApJ*, 654, 570
- Meixner, M. et al. 2006, *AJ*, 132, 2268
- Michie, D. Spiegelhalter, D., Taylor, C. 1994, in “Machine Learning, Neural and Statistical Classification”, Ellis Horwood Series in Artificial Intelligence, Ellis Horwood
- Oppenheimer, B. R., Kulkarni, S. R., Matthews, K. & van Kerwijk, M. H. 1998, *ApJ*, 502, 932
- Oppenheimer, B. R., Kulkarni, S. R., Matthews, K., van Kerwijk, M. H. 1995, *Science* 270, 1478
- Patten, B. M. et al. 2005, in “Protostars and Planet V”, proc. of the Conference held October 24-28, 2005, Hilton Waikoloa Village, The Big Island, Hawaii, LPI Contribution 1286, p. 8042
- Patten, B. M. et al. 2006, *ApJ*, 651, 502
- Pinfield, D. J. et al. 2008, *MNRAS*, in press, arXiv:0806.0294
- Roelling, T. L. et al. 2004, *ApJS*, 154, 418
- Simard, P., Le Cun, Y., Denker, J. 1993, in “Advances in Neural Information Processing Systems”, Morgan Kaufman, San Mateo, CA, p. 50
- Skrutskie, M. F. et al. 2006, *AJ*, 131, 1163
- Stern, D. et al. 2007, *ApJ*, 663, 677
- Storrie-Lombardi, L. J. & Silbermann, N. A. 2007, “The Science Opportunities for the Warm Spitzer Mission Workshop”, American Institute of Physics Conference Proceedings, vol. 943

Tarter, J. C. 1975, Ph.D. thesis (University of California, Berkeley)

Tinney, C. G., Burgasser, A. J., Kirkpatrick, J. D. & McElwain, M. W. 2005, *AJ*, 130, 2326

van der Veen, W. E. C. J., Habing, H. J. 1988, *A&A*, 194, 125

Werner, M. W. et al. 2004, *ApJS*, 154, 1

York, D. G. et al. 2000, *AJ*, 120, 1579

Table 1. Sample selection

Sample	N_{tot}	k -NN Colors Used
XFLS IRAC/2MASS	4,552	[3.6] – [4.5], [3.6] – [8.0], [4.5] – [5.8], J – [3.6], K_s – [4.5]
XFLS IRAC Warm	8,133	[3.6] – [4.5], J – [3.6], K_s – [4.5], $J - K_s$
Shallow Survey IRAC/FLAMEX	15,847	[3.6] – [4.5], [3.6] – [8.0], [4.5] – [5.8], J – [3.6], K_s – [4.5]
Shallow Survey IRAC Warm	71,590	[3.6] – [4.5], J – [3.6], K_s – [4.5], $J - K_s$

Table 2. k -NN efficiency and completeness optimization

	L/early-T		late-T		late-T (warm mission)	
	D_{th}	$\mathcal{C} = \mathcal{E}$	D_{th}	$\mathcal{C} = \mathcal{E}$	D_{th}	$\mathcal{C} = \mathcal{E}$
First Look Survey						
$k = 3$	0.62	93.1%	0.72	99.7%	0.68	99.3%
$k = 5$	0.74	90.3%	0.89	98.9%	0.87	98.3%
$k = 7$	0.83	87.7%	1.05	97.5%	1.06	95.9%
Shallow Survey & FLAMEX						
$k = 3$	0.56	89.7%	0.76	99.9%	0.63	97.8%
$k = 5$	0.68	85.2%	0.97	99.8%	0.81	95.3%
$k = 7$	0.76	83.3%	1.17	99.4%	0.99	92.2%

Table 3. k -NN search result

	k	D_{th}	N_{tot}	N_{sel}^{kNN}	\mathcal{E}'	N_{sel}^{opt}	$N_{sel}^{no\ opt}$
First Look Survey							
L/early-T	5	0.74	4,552	455	90.0%	1	2
late-T	5	0.89	4,552	45	99.0%	0	0
late-T (warm)	3	0.68	8,133	17	99.8%	0	0
Shallow Survey & FLAMEX							
L/early-T	5	0.68	15,847	2,831	82.1%	3	1
late-T	5	0.97	15,847	40	99.7%	1	0
late-T (warm)	3	0.63	71,590	1,582	97.8%	4	1

Table 4. XFLS brown dwarf candidates

#	RA	Dec	J	H	K	[3.6]	[4.5]	[5.8]	[8.0]	Type	Notes
1	260.38831	+59.27060	16.36	15.32	14.70	14.33	14.36	14.18	13.93	L/early-T	red star?
2	261.10120	+60.03591	15.74	15.06	14.77	13.96	13.97	14.03	14.00	L/early-T	
3	261.13129	+60.05562	16.59	16.05	15.20	14.59	14.42	14.52	14.36	L/early-T	galaxy?

Table 5. Shallow Survey brown dwarf candidates

#	RA [deg]	Dec [deg]	B_W	R	I	J	K	[3.6]	[4.5]	[5.8]	[8.0]	Type	Notes
1	216.278002	+34.355660	23.48	19.53	19.07	17.63	17.34	late-T	red galaxy?
2	216.603543	+34.140991	23.51	20.59	19.41	18.57	17.74	late-T	red galaxy?
3	217.032547	+34.098458	20.32	19.16	18.07	17.58	16.64	...	late-T	red galaxy?
4	217.462015	+33.503213	22.21	16.88	16.99	15.70	15.12	15.21	14.59	T4.5	J142950.9+333011
5	217.786508	+33.139283	...	22.75	20.40	17.38	16.30	15.80	15.69	15.35	15.12	L/early-T	
6	217.920577	+33.295865	27.24	22.30	20.04	17.42	16.41	15.79	15.69	15.52	15.88	L/early-T	
7	218.001634	+33.925557	...	26.00	22.33	19.29	18.63	17.70	17.22	16.32	...	late-T	red galaxy?
8	218.003005	+33.949375	...	23.89	21.35	18.89	18.80	17.79	17.46	16.90	16.07	late-T	red galaxy?
9	218.303091	+34.477201	26.43	21.69	19.23	16.33	15.20	14.58	14.69	14.47	14.42	L/early-T	
10	218.335896	+33.850797	20.25	18.86	17.12	17.01	16.40	15.21	L/early-T	bad I photometry?

Table 6. Companion search efficiency and completeness

	early-T		late-T	
	D_{th}	$\mathcal{C}\&\mathcal{E}$	D_{th}	$\mathcal{C}\&\mathcal{E}$
$d = 5$ pc	0.52	99.0%	0.57	97.2%
$d = 10$ pc	0.49	97.3%	0.55	97.1%
$d = 20$ pc	0.42	89.5%	0.52	96.3%

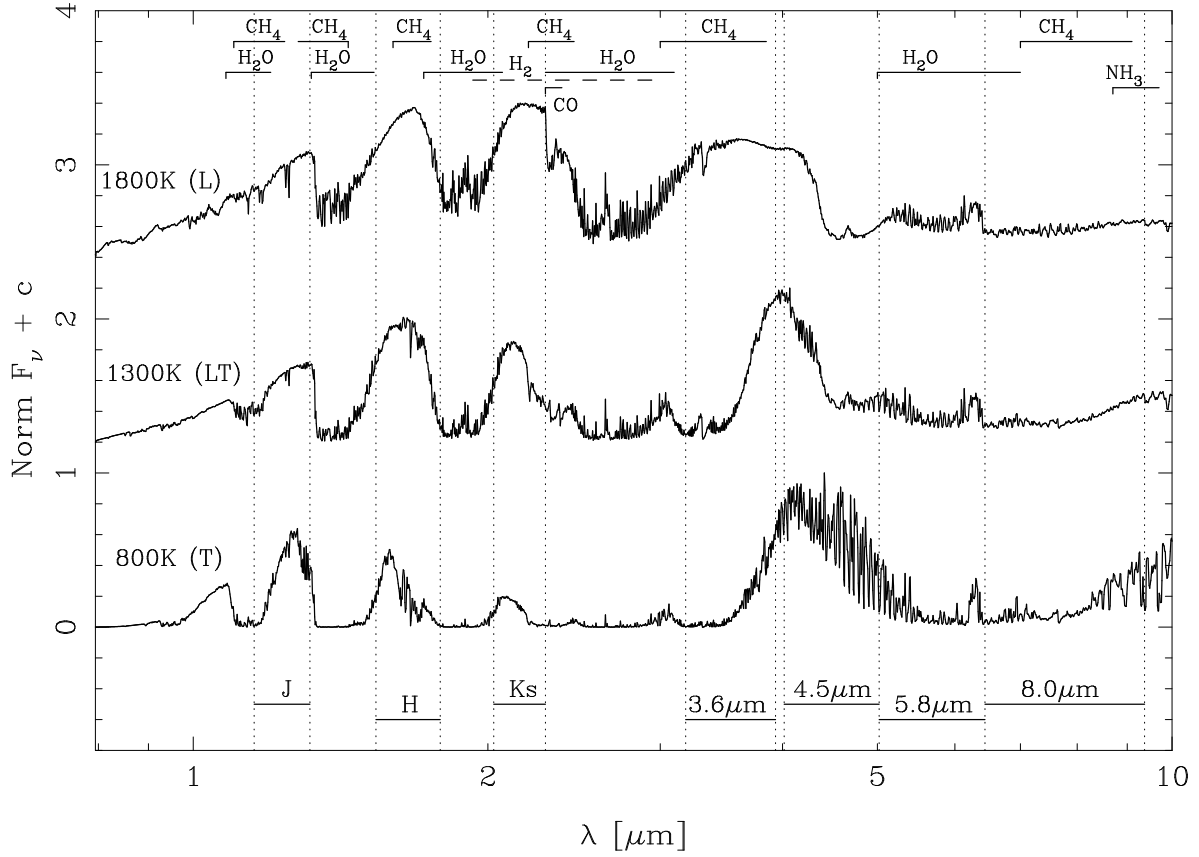


Fig. 1.— Model spectra of brown dwarfs with $T_{eff} \simeq 1800$ K (L dwarf), $\simeq 1300$ K (L-T dwarf transition) and $\simeq 800$ K (late T dwarf) from Burrows et al. (2006). The IRAC and 2MASS spectral band-passes are marked, as well as the main molecular absorption features in the near- and mid-IR range.

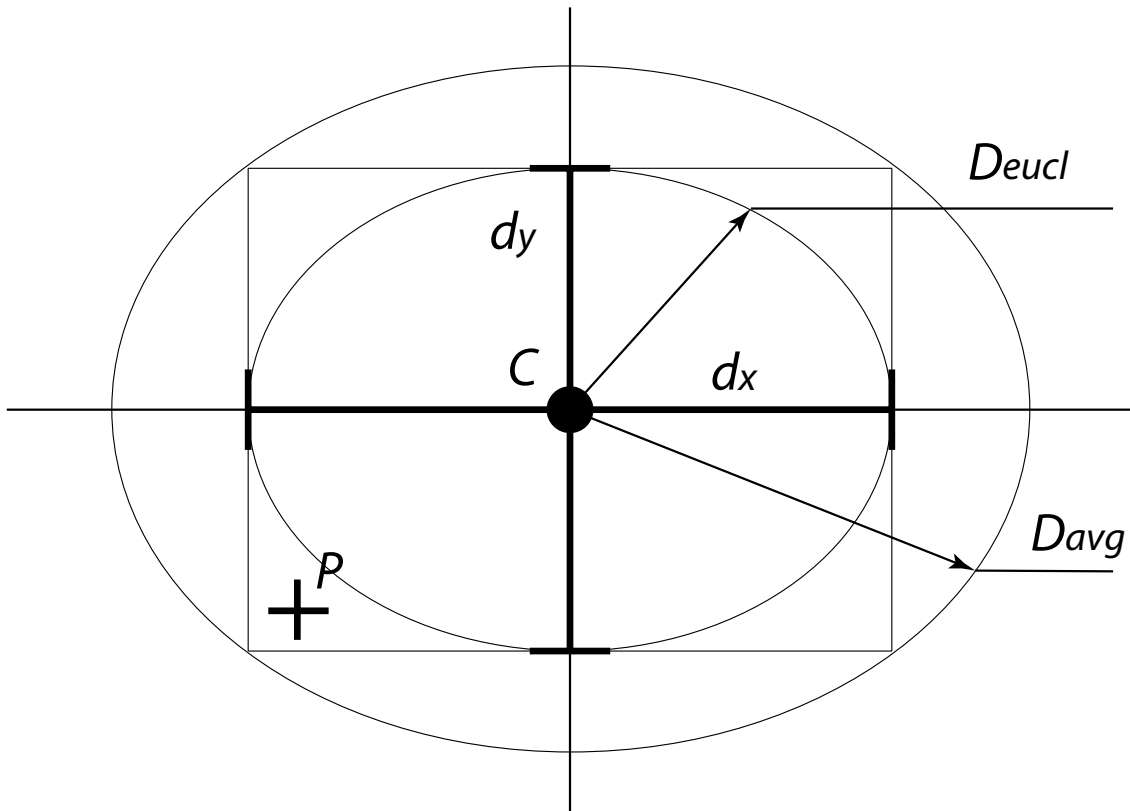


Fig. 2.— Effect of averaging in the metric. Assume that d_x and d_y are the distances in the two coordinates x and y . If the euclidean metric is adopted, the points in the x, y space with distance less than d_x and d_y in the two coordinates are included in the inner ellipse. If instead the euclidean metric is averaged in the two coordinates, any point within the larger ellipse will still have distance components less than d_x and d_y . The point P , having individual distances from the center C less than d_x and d_y will be excluded by the smaller ellipse but still included by the ellipse defined by the euclidean average metric.

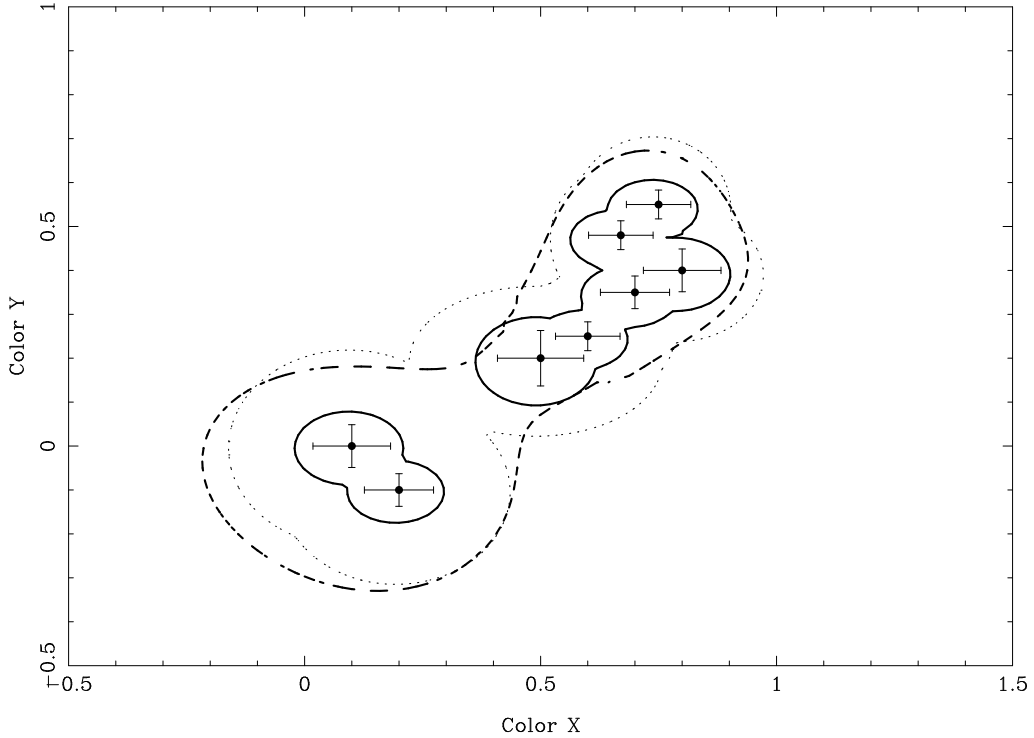


Fig. 3.— k -NN regions around their templates in a two-dimensional color-color diagram. The error bars for each template represent the total statistical error in equation 2. The solid line is the k -NN region for $k = 1$ and no systematic error $\sigma_s(j)$: note how the contour encloses the union of the individual regions represented in Figure 2 for $D_{avg} = 1$. The two templates at the bottom are separated enough from the others to form a disconnected region. When the sparseness of the templates $\sigma_s(j)$ is taken into account, a single region emerges (dotted line). For $k = 6$ the region contour becomes smoother, as shown by the dashed line. Note that for $k = 6$ the region around the isolated sources becomes wider, since $\sigma_s(j)$ is calculated reaching templates from the other group.

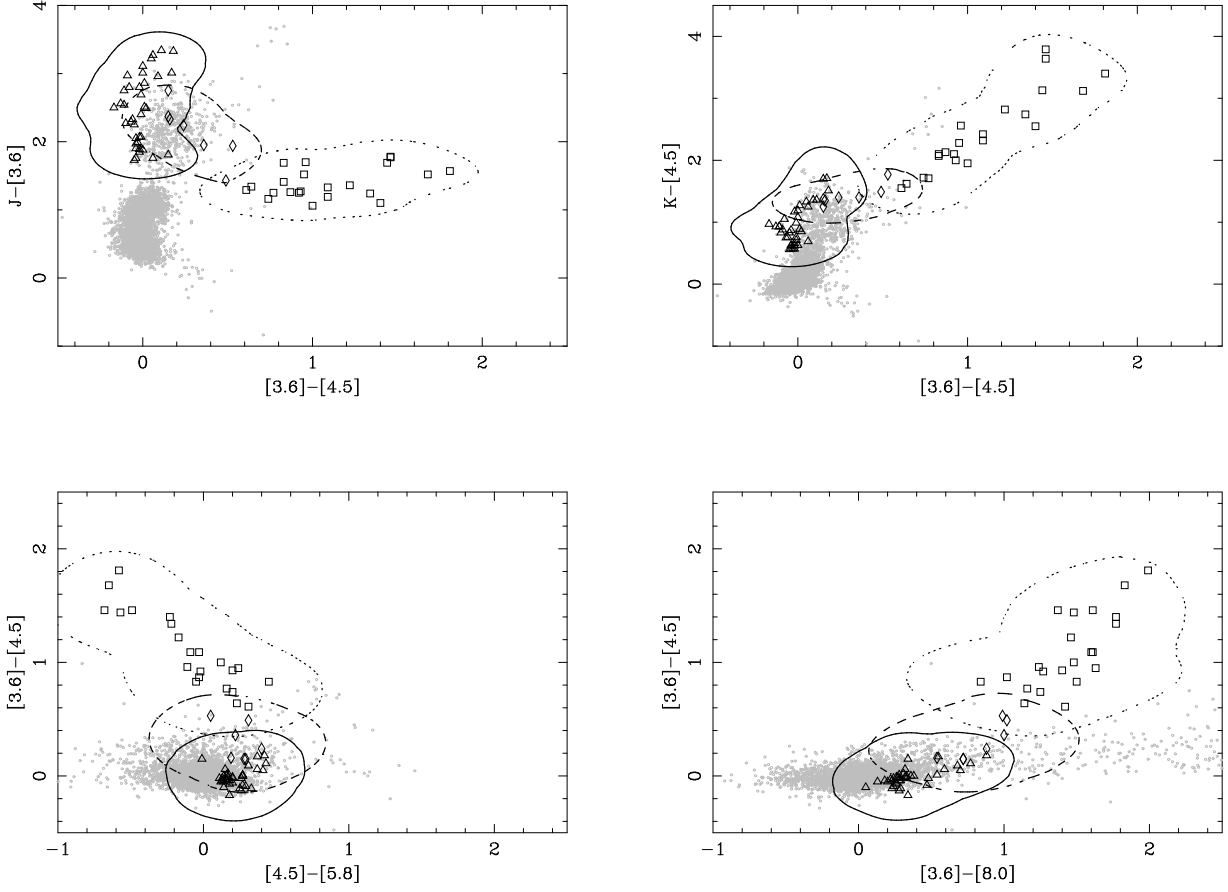


Fig. 4.— Grey points: *Spitzer* First Look Survey sources with good photometry ($S/N > 3$) in 6 bands (IRAC bands, plus J and K from the 2MASS survey). Triangles are Patten et al. (2006) L dwarfs, diamonds are early T dwarfs (spectral type $T < 4$) and squares are late T dwarfs (spectral type $T \geq 4$). Contours are the k -NN regions defined for $k = 5$ and $D_{kNN} = 1$ for L dwarfs (solid line), early T dwarfs (dashed line) and late T dwarfs (dotted line).

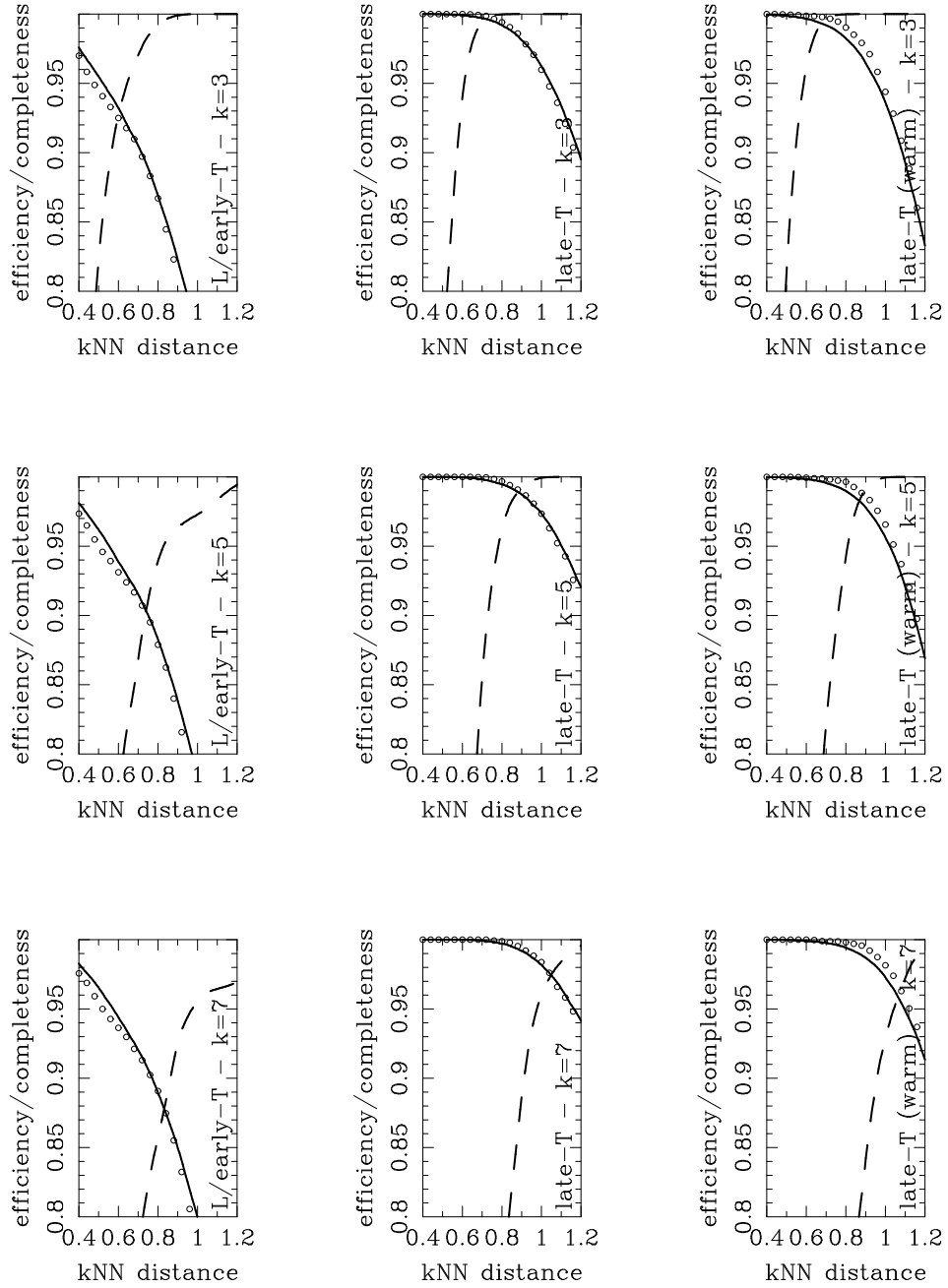


Fig. 5.— Predicted efficiency (solid line) and completeness (dashed line) of the L/early-T and late T search as a function of the k -NN distance threshold, for $k = 3, 5$ and 7 (using all colors or IRAC only colors). The prediction is based on a Monte Carlo simulation seeded with a 20% subsample of the First Look Survey database. The large dots are the actual fractions of sources rejected from the full datasets for different values of D_{th} .

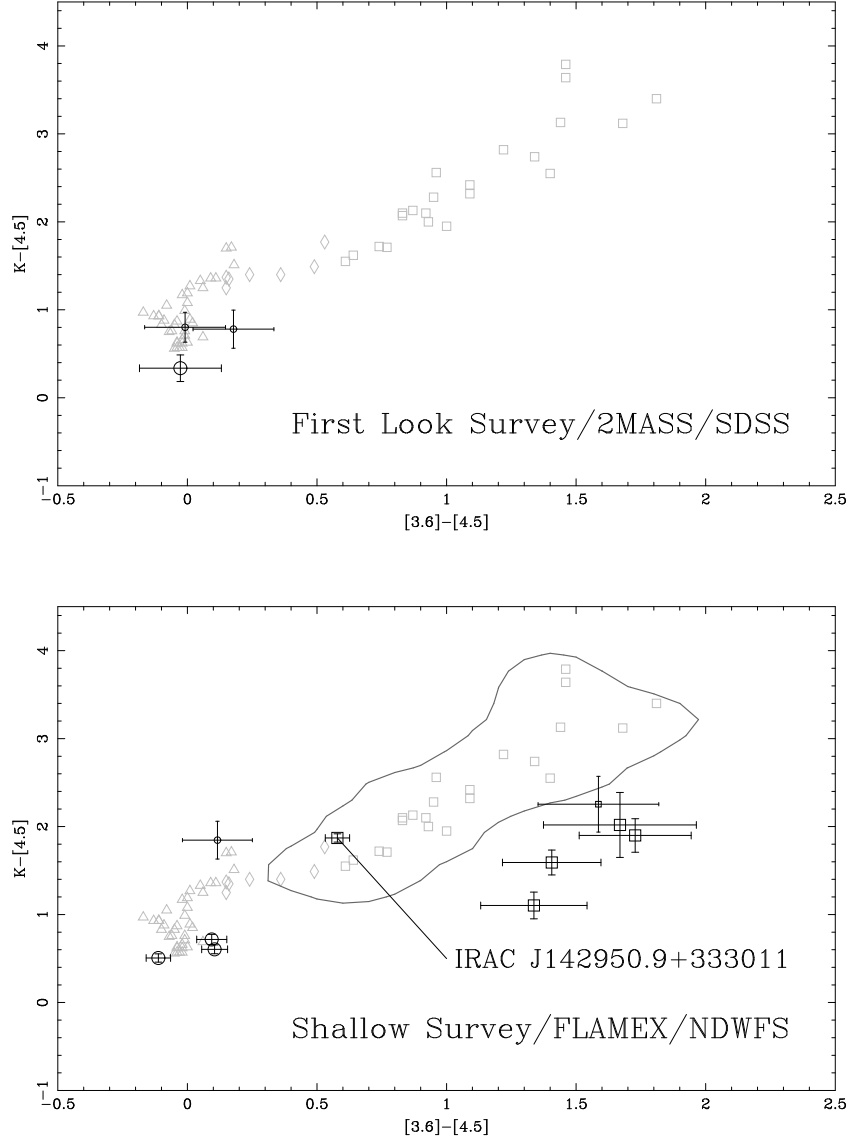


Fig. 6.— Best brown dwarf candidates for the First Look Survey (top) and the Shallow Survey/FLAMEX (bottom), selected using J , K and IRAC colors, satisfying the optical color requirement. Circles are L/early-T candidates and squares late-T candidates. Large symbols have been verified visually in the SDSS or NDWFS I band images to ensure they are single point sources and not extended sources or blends. Small symbols are not detected in the optical surveys. Grey symbols are the brown dwarf templates. The solid line in the bottom panel shows the k -NN region drawn for $k = 3$ and $D_{th} = 0.8$ using only the two variables in the plot ($K - [4.5]$ and $[3.6] - [4.5]$).

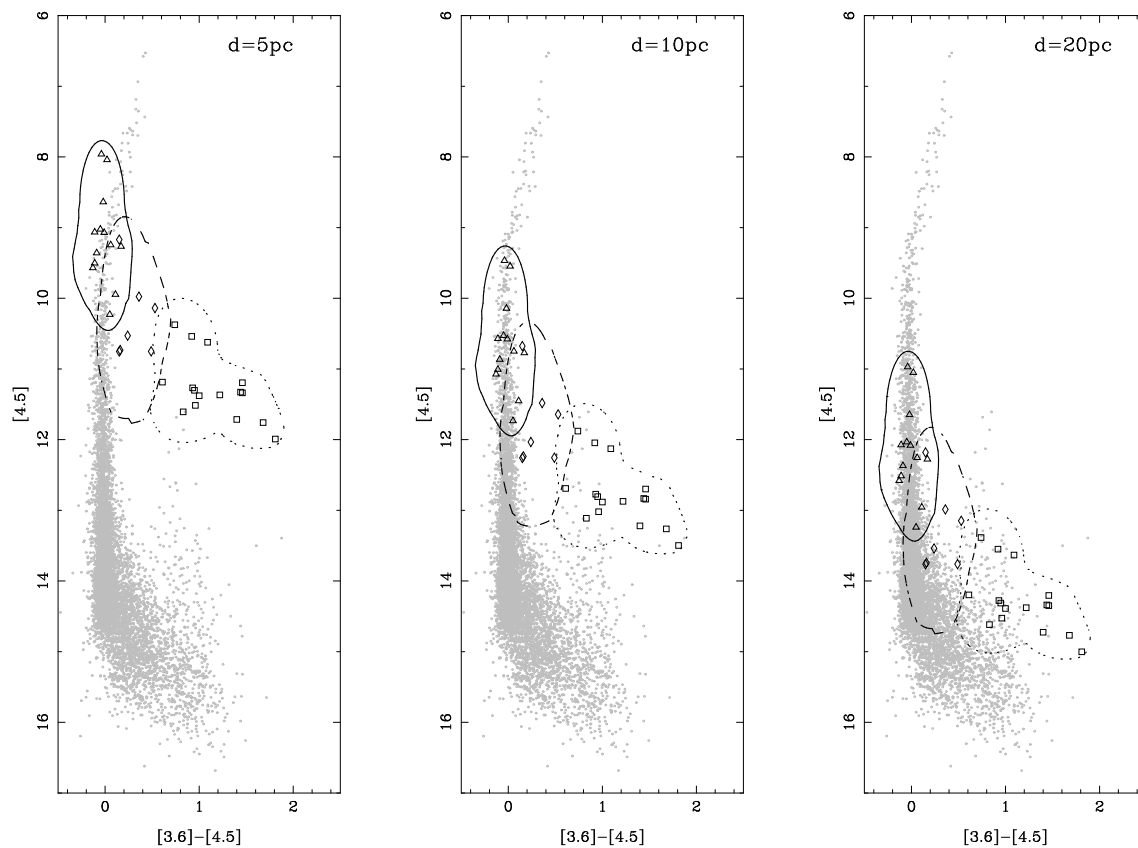


Fig. 7.— Color-magnitude diagram of simulated photometry around a nearby star. The data points are from the XFLS. The L, early T and late T template [4.5] magnitudes are computed for brown dwarfs at a distance of 5 (left), 10 (center) and 20 pc (right) respectively. The regions are plotted for $k = 5$. Symbols are the same as in previous plots.